Structural and Geometrical Isomerizations of Cyclopropane. Quantum Chemical and RRKM Calculations

Faina Dubnikova and Assa Lifshitz*

Department of Physical Chemistry, The Hebrew University, Jerusalem 91904, Israel

Received: December 11, 1997; In Final Form: February 20, 1998

Density functional theory and two-configuration self-consistent-field calculations were carried out to investigate the unimolecular isomerizations of cyclopropane. The calculated structural parameters and vibrational frequencies of cyclopropane are in good agreement with the measured values. Obtained structures and relative energies of the transition states for the geometrical (cis−trans) and optical isomerizations agree with previous calculations. A transition state for the structural isomerization cyclopropane → propylene was located, and its energy level and vibrational frequencies were calculated with uB3LYP/cc-pVDZ method. IRC calculations using the same method and basis set show that this transition state is connected to cyclopropane and propylene without an intermediate. The wave function of the transition state contains a contribution of ionic and biradical terms. The calculated activation energy and preexponential factor for k_∞ are in very good agreement with the experimental values. RRKM calculations of the first-order rate constant for the structural isomerization were carried out over a wide range of pressures and temperatures.

Introduction

During the past several decades a considerable effort has been devoted to the study of cyclopropane isomerizations both experimentally and theoretically.[1−4] Cyclopropane undergoes three types of isomerizations: geometrical, optical, and structural. In the geometrical and optical isomerizations, substituents such as methyl or other groups, or simply deuterium atoms in a partially deuterated cyclopropane, rearrange with respect to the ring's plane. Such a rearrangement requires rupture of a C−C σ-bond in the ring but no migration of H atom from one carbon atom to another takes place. In the structural isomerization, both bond cleavage and H-atom migration must occur.

Numerous quantum chemical calculations have been performed on cyclopropane, trying to localize transition states for the structural and geometrical isomerizations. Whereas a trimethylene intermediate and a number of transition states for the geometrical and optical isomerizations have been successfully calculated by many investigators[2,5−12] we are aware of only one recent study[13] reporting on ab initio calculations of transition states for two reactions, trimethylene → cyclopropane and trimethylene → propylene, which can be viewed together as the reaction path for the structural isomerization of cyclopropane. We also found a rather old semiempical SINDO study[14] where such a saddle point for the structural isomerization was located. The estimated activation energy for this isomerization was 48 kcal/mol, which deviated from the experimental value by about 15 kcal/mol.

The question whether the structural isomerization proceeds via a concerted or a stepwise mechanism involving a biradical intermediate has also been addressed by unimolecular rate theories. Whereas early studies[15−18] gave preference to the concerted mechanism it was later obvious that a stepwise mechanism could not be ignored.[16,19,20]

In the present study, we report on ab initio and density functional theory calculations of the transition state for the reaction path in the unimolecular structural isomerization of cyclopropane, cyclopropane → propylene. We also report on calculations of the geometrical rearrangements by the same methods for comparison with previous studies. Density functional theory has never been applied to this system in the past.

Whereas propylene is the only product of the structural isomerization of cyclopropane, the structural isomerization of derivatives of cyclopropane yield several products. For example, structural isomerization of cyclopropanecarbonitrile yields *cis*- and *trans*-crotonitrile ($CH_3CH{=}CHCN$), vinylacetonitrile ($CH_2{=}CHCH_2CN$), and methacrylonitrile ($CH_2{=}C(CH_3)CN$). This reaction was studied experimentally both at low[21] and at high temperatures using the single-pulse shock tube technique.[22] The quantum chemical and model calculations of these reactions will be reported separately.

Computational Details

Optimization of the ground-state geometry of cyclopropane and propylene, the geometry of trimethylene, and the transition states of the reactions under consideration was carried out using density functional theory (DFT) employing the Becke three-parameter hybrid method (B3LYP,[23] with Lee−Yang−Parr correlation functional approximation[24]) by means of the Berny geometry optimization algorithm. The DFT computations were carried out using the Gaussian-94 program package.[25]

We have tested several methods and several basis sets before choosing the method and basis set for the present calculations. In addition to DFT, MP2 calculations with the frozen core approximation were carried out. Three basis sets were tested with these methods: the standard Pople polarized split-valence 6-31G**[26] and the Dunning correlation consistent polarized valence double ζ (cc-pVDZ) and triple ζ (cc-pVTZ) basis sets.[27,28] All the calculations were performed without symmetry restrictions. Vibrational analyses were carried out at the same levels of theory to characterize the optimized structures as local minima or transition states. Each optimized structure was

S1089-5639(98)00503-9 CCC: $15.00
Published on Web 04/22/1998

TABLE 1: Comparison of Observed and Calculated Structural Parameters of Cyclopropane at Different Computational Levels

parameter[a]	r-C−C	r-C−H	∠CCC	∠HCH
experimental[b]	1.514(1)[c]	1.099(2)	60.0	114.5(9)
HF/6-31G**	1.497	1.076	60.0	114.1
HF/cc-pVDZ	1.500	1.083	60.0	114.3
MP2/6-31G**	1.500	1.079	60.0	114.4
MP2/cc-pVDZ	1.513	1.092	60.0	114.7
B3LYP/6-31G**	1.509	1.086	60.0	114.0
B3LYP/cc-pVDZ	1.511	1.093	60.0	114.2
B3LYP/cc-pVTZ	1.505	1.081	60.0	114.2

[a] Distances in angstroms, angles in degrees. [b] Experimental parameters from ref 33. [c] Values in parentheses denote standard deviations and apply to the last digits of the constants.

recalculated at single-point quadratic CI calculations including single and double substitutions with a triplet contribution to the energy—QCISD(T)[29]. QCISD(T) calculations were performed with frozen core approximation.

Biradical structures were localized by using guess wave function with the destruction $\alpha-\beta$ and spatial symmetries by the unrestricted uB3LYP method and were recalculated also by the single-point uQCISD(T) method.

We used an open-shell singlet approximation for calculating the various intermediates and transition states for two reasons: (1) The ground state of cyclopropane is a singlet and spin conservation requires that the biradicals should be, at least initially, in the singlet state.[3] (2) There is experimental evidence that triplet-derived trimethylenes lead to the formation of products resulting from geometrical isomerizations but no propylenes are produced, whereas singlet-derived trimethylenes give substantial amounts of both products.[30]

Since the DFT methods are less sensitive to multireference effects, all the structures were also fully optimized using the two-configuration self-consistent-field (TCSCF) method with the cc-pVDZ basis set. The reference configuration was defined by filling separately the α and β occupied orbitals (six singlet configurations). The initial guess wave functions were taken from unrestricted Hartree−Fock (uHF) calculations at optimal uB3LYP geometry. The TSCSF calculations were carried out using the Gamess-USA program.[31]

Calculated vibrational frequencies and entropies (at uB3LYP and TCSCF levels) were used to evaluate preexponential factors of the reactions under consideration. All the calculated frequencies as well as the zero point energies are of harmonic oscillators. The calculated frequencies were not scaled. The calculations of the intrinsic reaction coordinate (IRC) were done at the uB3LYP level of theory with mass-weighted internal coordinates, to make sure that the transition states connect the desired reactants and products. Only this coordinate system permits us to follow to steepest descent path.[32] We computed the IRC path using the same basis set that was used for the stationary point optimization.

All the calculations were done on a DEC Alpha TurboLaser 8200 5/300 at the Institute of Chemistry of The Hebrew University of Jerusalem.

Results and Discussion

Table 1 shows selected experimental[33] and calculated parameters of cyclopropane using the B3LYP, MP2, and HF levels of theory with two basis sets, 6-31G** and cc-pVDZ. (The triple ζ (cc-pVTZ) basis set was used only with the B3LYP method.) As can be seen, the geometry of cyclopropane when calculated with the cc-pVDZ basis set for each level of theory is in better agreement with the experimental structure than when calculated using 6-31G**. The use of the triple ζ basis set did not improve the results.

TABLE 2: Experimental and Calculated Frequencies of Cyclopropane (in cm^{-1}) Using Different Methods

	B3LYP/cc-pVDZ			MP2/cc-pVDZ			
expt[a]	raw	Δraw[b] (%)	Δscale[b,c] (%)	raw	Δraw[b] (%)	Δscale[b,d] (%)	mode description[e]
739*	729	−1.4	−5.1	738	−6.8	−14.9	CH_2 s stretch
854	853	−0.1	−4.0	861	−4.1	−4.9	CH_2 s scis
867*	888	2.4	−1.5	918	−5.7	−0.1	ring stretch
1028*	1043	1.4	−0.2	1062	−0.9	−3.9	CH_2 twist
1070	1070	0	−3.9	1078	6.0	−5.0	CH_2 wag
1126	1136	0.9	−3.0	1162	3.7	−2.7	CH_2 a stretch
1188*	1195	0.6	−3.2	1211	4.9	−3.8	CH_2 rock
1188	1218	2.5	−1.4	1243	7.8	−1.3	CH_2 s stretch
1438*	1440	0.1	−3.7	1466	6.5	−3.8	CH_2 scis
1479	1498	1.3	−2.6	1530	6.8	−2.4	CH_2 wag
3024*	3120	3.2	−0.8	3192	5.2	−0.4	ring deform
3038	3129	3.0	−0.9	3203	5.1	−0.5	CH_2 a stretch
3082*	3203	3.9	−0.1	3290	3.7	0.7	CH_2 twist
3102	3224	3.9	−0.1	3309	5.3	0.6	CH_2 rock

[a] Experimental frequencies from ref 32. [b] Δ = (calculated value − experimental value)/experimental value in percent. [c] Scaling factor is 0.9613.[33] [d] Scaling factor is 0.9434.[33] [e] Mode descriptionfrom ref 7. * doubly degenerate.

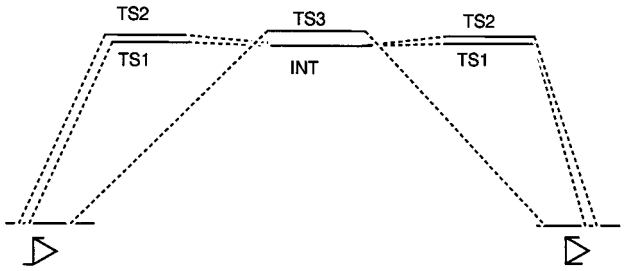

Figure 1. Schematic presentation of the stepwise and concerted channels of the geometrical and optical isomerizations of cyclopropane.

Table 2 shows experimental and calculated frequencies of cyclopropane for two best combinations of methods and basis sets, i.e., MP2/cc-pVDZ and B3LYP/cc-pVDZ. The B3LYP/cc-pVDZ frequencies are in better agreement with the measured values.[33] The scaling of the calculated frequencies[34] did not improve the agreement with the experiment. On the contrary, the percent deviations of the unscaled (raw) frequencies were smaller. We have thus chosen the B3LYP method and cc-pVDZ basis set for all our calculations without frequency scaling. The same basis set was also used with the TCSCF method.

Geometrical and Optical Isomerizations. Recently, Baldwin et al.[8] and Doubleday[13] calculated transition states for the geometrical and optical isomerizations of cyclopropane. Baldwin et al. used TCSCF and SCF levels of theory with configuration interaction at the SCF-optimized geometry. Doubleday used a complete active space multiconfiguration self-consistent field (CASSCF) with 2,2-CAS and 4,4-CAS wave functions. The conclusions, which were based on these and other quantum chemical calculations, as well as on a kinetic isotope effect,[8] suggested that the geometrical and optical isomerizations can be described by three competitive paths with several distinct conformers in the trimethylene system. The three computed competitive paths are shown in Figure 1.

Our calculated uB3LYP and TCSCF transition states of the ring-opening TS1 and TS2, and trimethylene biradical as a short-living intermediate, INT, are shown in Figure 2. These three structures are edge-to-edge (EE or "0,0") conformers of trimethylene. The geometrical parameters are shown in Tables 3

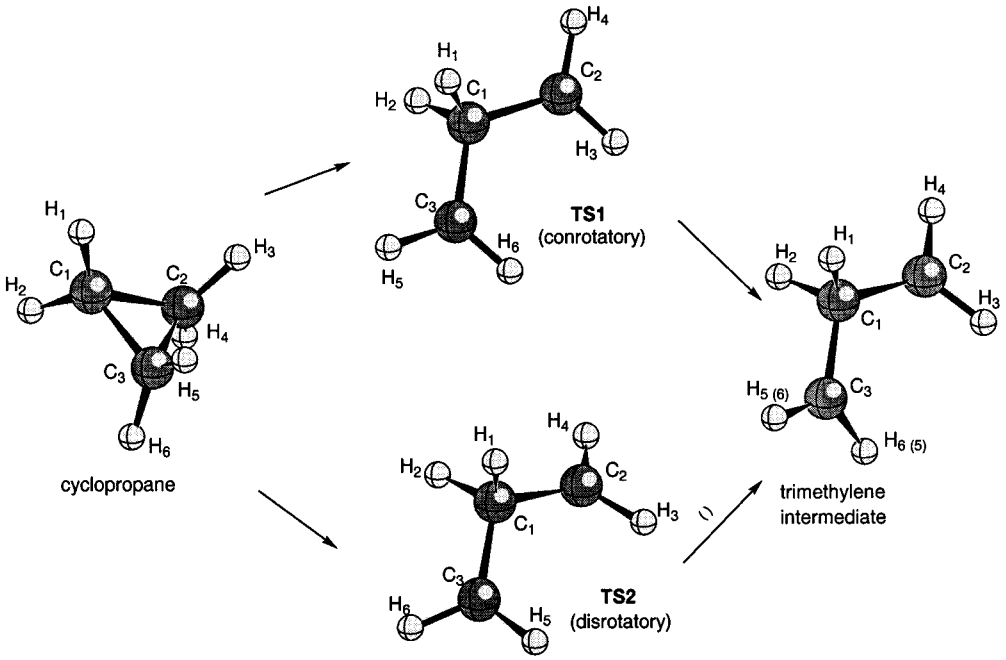

Figure 2. Optimized structures of the transition states TS1 (conrotatory) and TS2 (disrotatory) and the intermediate for the two channels of the geometrical isomerization.

TABLE 3: Structural Parameters of All the C_3H_6 Species at the uB3LYP Level of Theory

parameter[a]	CPR[b]	TS1	TS2	T3	INT	TS4	TS5	propylene
r−C(1)C(2)[c]	1.511	1.490	1.500	1.498	1.491	1.421	1.445	1.336
r−C(1)C(3)	1.511	1.490	1.500	1.501	1.491	1.483	1.375	1.501
r−C(2)C(3)	1.511	2.541	2.492	2.523	2.532	2.611	2.354	2.521
∠C(2)C(1)C(3)	60.00	117.02	112.39	114.46	116.26	128.06	113.16	125.35
r−H(1)C(1)	1.093	1.116	1.119	1.115	1.115	1.181	1.604	2.161
r−H(2)C(1)	1.093	1.116	1.104	1.108	1.115	1.099	1.097	1.098
∠H(1)C(1)H(2)	114.21	102.05	104.51	104.40	102.62	104.94	84.14	55.50
r−H(3)C(2)	1.093	1.092	1.092	1.093	1.092	1.090	1.091	1.093
r−H(4)C(2)	1.093	1.093	1.094	1.094	1.093	1.093	1.092	1.095
∠H(3)C(2)H(4)	114.21	118.40	118.27	117.97	118.43	118.28	117.98	116.99
r−H(5)C(3)	1.093	1.093	1.092	1.094	1.093	1.090	1.098	1.105
r−H(6)C(3)	1.093	1.092	1.093	1.092	1.092	1.093	1.094	1.101
∠H(5)C(3)H(6)	114.23	118.40	118.29	118.63	118.43	118.61	117.99	108.16
∠H(1)C(1)C(2)	118.06	109.20	109.68	109.41	109.52	107.70	130.72	135.11
∠H(1)C(1)C(3)	118.07	109.18	109.62	108.68	109.03	74.68	88.99	28.48
∠H(2)C(1)C(2)	118.06	109.16	110.21	110.13	109.03	115.41	117.75	118.67
∠H(2)C(1)C(3)	118.05	109.19	110.15	109.27	109.52	113.60	117.50	115.97
∠H(3)C(2)C(1)	118.06	120.08	121.48	121.30	120.38	119.76	118.43	121.55
∠H(4)C(2)C(1)	118.06	121.51	120.08	120.18	121.03	121.33	120.92	121.46
∠H(5)C(3)C(1)	118.04	121.51	121.27	119.92	121.03	118.28	122.48	111.11
∠H(6)C(3)C(1)	118.06	120.09	120.15	121.26	120.38	119.79	119.53	117.70
τH(3)C(2)C(1)C(3)	107.90	0.69	43.64	99.92	19.60	15.21	61.11	0.00
τH(4)C(2)C(1)C(3)	−107.95	−179.67	−141.17	−71.46	−165.01	−174.10	−132.79	−179.97
τH(5)C(3)C(1)C(2)	107.90	−179.51	41.37	12.44	19.64	177.97	27.03	120.86
τH(6)C(3)C(1)C(2)	−107.95	0.61	−144.91	−172.62	−165.03	18.81	−153.10	0.00

[a] Distances in angstroms, angles in degrees. [b] Cyclopropane. [c] Atom numbers are shown in Figures 2−4.

(uB3LYP-optimized) and 4 (TCSCF-optimized). As can be seen, both methods show the same variation in the geometrical parameters along the reaction paths. Both the C−C and C−H distances obtained by the TCSCF optimization are somewhat longer and the angles are somewhat smaller. Note that in the two tables H(5) and H(6) in the trimethylene intermediate should be interchanged depending upon whether it is produced via TS1 (conrotatory) or TS2 (disrotatory) paths.

The reaction coordinate in TS1 is a conrotatory double rotation of the terminal methylene groups and in TS2 it is disrotatory. In TS3 it is a single rotation of a terminal methylene group about the C(1)−C(2) (or C(3)−C(2)) bond. This edge-to-face (EF or "0,90") conformer of trimethylene (Figure 3), TS3, was localized as a transition state at TCSCF level but as a second-order stationary point structure, T3, at uB3LYP level of theory. The frequencies, including the imaginary ones, of all the C_3H_6 species are shown in Table 5. The edge-to-face (EF) and face-to-face (FF or "90,90") species of trimethylene either as a local minimum or a transition state could not be localized at uB3LYP level.

It is of interest to compare our calculated transition states and trimethylene intermediate to those of Baldwin et al.[7,8] and Doubleday[13] (See Table 9, where the methods and the basis sets are given). Note that our transition state TS1 is C_1(ts) in Baldwin calculations and $1^{\#}$ in Doubleday's, TS2 is C_s(ts) and $2^{\#}$, and TS3 is EF(ts) and 4, respectively. Our notation of the trimethylene intermediate is INT, it is C_s(int) in Baldwin's calculations and 1 or 2 in Doubleday's.

TABLE 4: Structural Parameters of C_3H_6 Species at the TCSCF Level of Theory

parameter[a]	TS1	TS2	TS3	INT	TS4
r−C(1)C(2)[b]	1.501	1.506	1.507	1.502	1.407
r−C(1)C(3)	1.501	1.506	1.507	1.502	1.481
r−C(2)C(3)	2.538	2.478	2.535	2.520	2.602
∠C(2)C(1)C(3)	115.38	110.68	114.52	114.11	128.53
r−H(1)C(1)	1.100	1.100	1.098	1.098	1.187
r−H(2)C(1)	1.097	1.093	1.095	1.098	1.085
∠H(1)C(1)H(2)	104.82	105.71	105.43	105.18	106.86
r−H(3)C(2)	1.083	1.083	1.089	1.083	1.079
r−H(4)C(2)	1.084	1.084	1.084	1.083	1.083
∠H(3)C(2)H(4)	116.73	117.11	116.64	117.02	118.12
r−H(5)C(3)	1.082	1.082	1.084	1.083	1.080
r−H(6)C(3)	1.081	1.084	1.083	1.083	1.082
∠H(5)C(3)H(6)	117.97	117.13	114.52	117.02	118.40
∠H(1)C(1)C(2)	108.68	110.72	108.61	109.15	107.55
∠H(1)C(1)C(3)	108.83	110.74	108.83	109.43	67.95
∠H(2)C(1)C(2)	109.23	109.46	109.75	109.43	116.24
∠H(2)C(1)C(3)	109.38	109.41	109.30	109.15	117.71
∠H(3)C(2)C(1)	118.95	120.41	119.90	119.46	119.75
∠H(4)C(2)C(1)	119.65	119.24	118.95	119.51	121.50
∠H(5)C(3)C(1)	121.34	120.36	118.38	119.51	117.86
∠H(6)C(3)C(1)	119.78	119.31	120.21	119.49	119.76
τH(3)C(2)C(1)C(3)	37.77	50.68	69.21	41.41	13.56
τH(4)C(2)C(1)C(3)	−167.23	−150.20	−86.18	−161.76	−175.75
τH(5)C(3)C(1)C(2)	167.57	48.61	17.34	41.40	174.13
τH(6)C(3)C(1)C(2)	−1.24	−152.16	−173.04	−161.76	16.95

[a] Distances in angstroms, angles in degrees. [b] Atom numbers are shown in Figures 1−4.

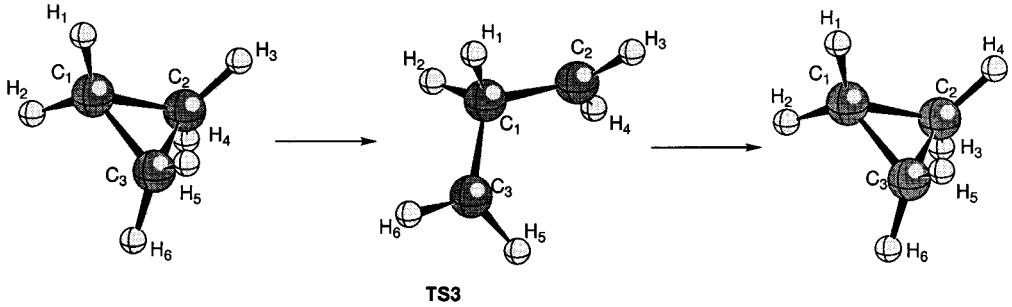

Figure 3. Optimized structure of the transition state TS3 for the concerted geometrical isomerization channel.

TABLE 5: uB3LYP/cc-pVDZ and TCSCF/cc-pVDZ Frequencies of the Different C_3H_6 Species (in cm^{-1})[a]

	uB3LYP/cc-pVDZ
TS1	(i-107), 143, 367, 414, 417, 786, 888, 900, 1114, 1125, 1130, 1335, 1386, 1427, 1449, 2898, 2910, 3140, 3142, 3252, 3252
TS2	96, (i-290), 323, 419, 464, 747, 886, 949, 1093, 1154, 1164, 1339, 1424, 1427, 1444, 2856, 3041, 3134, 3137, 3248, 3249
T3	(i-51), (i-254), 325, 374, 502, 744, 891, 985, 1071, 1100, 1226, 1317, 1417, 1427, 1447, 2913, 2994, 3130, 3160, 3247, 3248
INT	27, 197, 376, 419, 421, 759, 901, 929, 1081, 1126, 1167, 1331, 1388, 1428, 1448, 2909, 2913, 3138, 3141, 3251, 3252
TS4	342, 398, 529, 575, 598, 801, 907, 932, 1168, 1230, 1247, 1388, (i-1423), 1444, 1503, 2424, 3111, 3146, 3150, 3259, 3266
TS5	245, 441, 564, 585, 665, 850, 912, 1008, 1044, 1103, 1188, 1251, 1389, 1437, 1593, (i-1842), 3113, 3132, 3148, 3240, 3253
	TCSCF/cc-pVDZ
TS1	(i-202), 220, 323, 374, 551, 848, 945, 998, 1178, 1193, 1290, 1475, 1561, 1569, 1587, 3124, 3174, 3272, 3291, 3385, 3391
TS2	251, (i-297), 331, 505, 526, 851, 914, 1026, 1154, 1264, 1315, 1480, 1577, 1585, 1612, 3100, 3200, 3296, 3316, 3390, 3412
TS3	169, (i-288), 370, 489, 621, 786, 951, 1086, 1155, 1165, 1364, 1456, 1565, 1577, 1593, 3135, 3176, 3282, 3292, 3390, 3395
INT	186, 306, 386, 519, 533, 803, 951, 1077, 1137, 1175, 1328, 1479, 1559, 1571, 1584, 3120, 3163, 3283, 3299, 3386, 3394
TS4	354, 431, 555, 621, 661, 900, 971, 1010, 1269, 1341, 1352, 1517, 1574, (i-1596), 1653, 2499, 3302, 3310, 3331, 3419, 3428
TS5	297, 424, 542, 598, 644, 836, 1029, 1103, 1162, 1189, 1295, 1377, 1511, 1589, 1693, (i-2072), 3161, 3194, 3219, 3313, 3325

[a] Imaginary frequencies are shown in parentheses.

The main difference between our calculation and Doubleday's[13] is the number of intermediates that participate in the geometrical isomerization manifold. Whereas Doubleday found two distinct intermediates for transition states $1^{\#}$ and $2^{\#}$, both our calculations and Baldwin's[7,8] point to the existence of one single intermediate. An additional important point is the nature of TS3 (EF(ts) in Baldwin's calculation and 4 in Doubleday's). Baldwin et al.[7,8] claim that their EF(ts) is a saddle point, whereas Doubleday[13] got a second-order stationary point, both using TCSCF. Our TCSCF calculations show that TS3 is a transition state, but uB3LYP, on the other hand, shows that it is only a second-order stationary point. This disagreement remains an open question.

It can be shown that the geometrical isomerization (cis−trans) proceeds with respect to central and terminal group if the reaction goes via TS1 and TS2 (Figures 2 and 3). This argument is true provided that there is no transition from TS1 to TS2 or TS2 to TS1 along the reaction coordinate. However, if such a transition does occur, then the cis−trans isomerization proceeds with respect to the two terminal methylene groups similar to the TS3 path.

In all the trimethylene intermediates and in the transition states there is a complete C−C bond rupture (see r-C(2)C(3) and ∠C-(2)C(1)C(3) in Tables 3 and 4). Some pyramidalization of the central methylene group takes place which expresses itself by

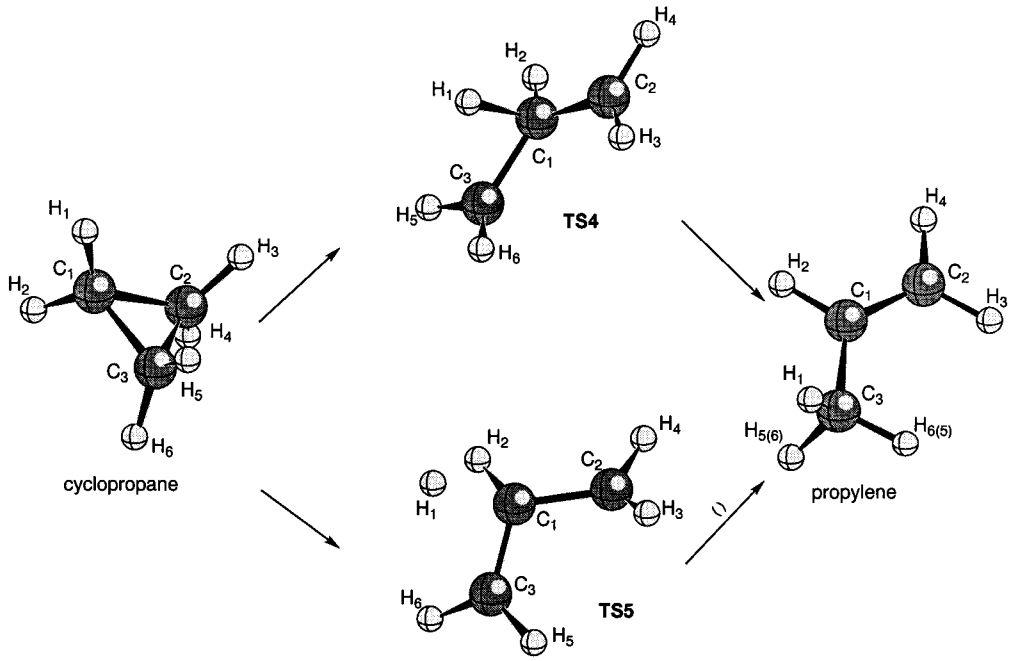

Figure 4. Optimized structures of the transition states TS4 and TS5 of two channels of the structural isomerization.

TABLE 6: Atomic Spin Densities of Trimethylene Conformers at the uB3LYP/cc-pVDZ Level[a]

	C(1)	C(2)	C(3)	H(1)	H(2)	H(3)	H(4)	H(5)	H(6)
TS1	0.00	1.05	−1.05	0.00	0.00	−0.04	−0.04	0.04	0.04
TS2	0.00	1.05	−1.05	0.00	0.00	−0.04	−0.04	0.04	0.04
T3	0.00	1.06	−1.03	−0.03	−0.03	−0.04	−0.04	0.04	0.05
INT	0.00	1.12	−1.12	0.01	−0.01	−0.01	−0.01	0.01	0.01
TS4	−0.10	0.68	−0.67	0.09	0.00	−0.02	−0.02	0.03	0.03

[a] Positive number indicates an excess α-spin occupancy. Negative number indicates an excess β-spin occupancy

change in the angles H(1)C(1)C(2), H(2)C(1)C(3), H(2)C(1)C-(2), and H(3)C(1)C(3) from 120° to about 109−110°. The biradical character of the trimethylenes can be seen from the coefficients of occupancy of the main configuration which are obtained at TCSCF level of theory. The values are 110 = 0.997 in TS1, 110 = 0.977 in TS2, 110 = 0.970 in TS3, and 110 = 0.959 in the intermediate, where 110 is the configuration of the single occupied orbitals with α and β spin, respectively, and the vacant orbital. The analysis of the distribution of atomic spin densities (Table 6) that was obtained at the uB3LYP level of theory leads to the same conclusion. The spin contamination of the uB3LYP wave functions (Table 7) also shows that these structures are "spin-contaminated structures". Further analysis of the molecular orbitals may explain the deviation of the dihedral angles (see Tables 3 and 4) from the plane of the carbon atoms. This deviation may be associated with less attraction of the lone pairs of the terminal carbons atoms, which consist of the frontier orbital.

The calculated energies of the intermediate and the transition states at different levels of theory and the relative energies with respect to cyclopropane are shown in the Table 8. Table 9 shows the results in comparison to Baldwin's[7,8] and Doubleday's[13] calculations, where the relative energies are given with respect to the trimethylene intermediate. As can be seen, the agreement of our calculations with those of Baldwin and Doubleday is very good. Zero point energies are not shown in the table. With zero point energies (Table 8), the energy level of the conrotatory transition state becomes either equal to or lower than the intermediate. All the transition states are

TABLE 7: Molecular Parameters of C_3H_6 Species Calculated Using Two Different Computational Methods

	moments of inertia[a]						
	$A \times 10^{38}$	$B \times 10^{38}$	$C \times 10^{38}$	μ^b	S^c	ZPE[d]	$\langle S^2 \rangle^e$
			uB3LYP/cc-pVDZ				
CPR[f]	4.1976	4.1992	6.7057	0.00	60.282	50.56	
TS1	2.1894	8.8882	10.5735	0.39	65.801	44.99	0.9848
TS2	2.3899	8.7462	10.2218	0.32	66.647	45.17	1.0001
T3	2.3713	8.9335	10.2356	0.21	63.175	45.03	1.0068
INT	2.2183	8.8834	10.4888	0.40	71.182	45.17	0.9842
TS4	1.7748	9.3375	10.6370	1.13	63.563	44.91	0.4756
TS5	2.4136	8.0963	9.4934	2.34	63.860	43.12	
			TCSCF/cc-pVDZ				
TS1	2.2191	8.9190	10.5092	0.47	64.784	48.24	
TS2	2.3790	8.7034	10.1943	0.48	64.148	48.76	
TS3	2.3917	8.8993	10.2117	0.25	64.620	48.63	
INT	2.2487	8.7403	10.3620	0.43	65.801	48.95	
TS4	1.7127	9.2464	10.7275	1.13	62.912	47.90	

[a] Moments of inertia (in g cm^2). [b] Dipole moments (in Debye). [c] Entropy in (cal/mol·kelvin). [d] Zero point energy (in kcal/mol). [e] Spin contamination at the uB3LYP level of theory. [f] Cyclopropane.

practically equal in energy, the lowest being TS1, the conrotatory transition state. This behavior was also found in previous calculations.

Structural Isomerization. The structural isomerization of cyclopropane is associated with both C−C bond cleavage and H-atom migration (Figure 4). The geometrical parameters of the calculated transition states TS4 and TS5 are summarized in Tables 3 and 4. The C(2)−C(3) distance in TS4 is roughly the same as in TS1, in TS2, and in the biradical intermediate of the geometrical isomerization manifold. However, the C(2)C-(1)C(3) angle is considerably wider than the equivalent one in the geometrical isomerization. It is 128° compared to approximately 115°. H(1) in the transition state TS4 is further away from C(1) as compared to the same distance in cyclopropane (r-H(1)C(1) ∼ 1.18 Å in TS4 and 1.093 Å in cyclopropane). The distances C(1)−C(2) and C(1)−C(3) indicate where the location of the double and the single bonds in propylene are formed. The reaction coordinate is a combination of two normal modes: 1,2 H-atom shift together with an asymmetric stretch of the carbon ring (Figure 4).

TABLE 8: Total Energies E_{total} (in a.u.), Relative Energies ΔE_{total}, and $\Delta E^{\ddagger a}$ (in kcal/mol) of All the Calculated C_3H_6 Species at Different Computational Levels

	uB3LYP			uQCISDT			TCSCF		
	E_{total}	ΔE_{total}	$\Delta E^{\ddagger}$	E_{total}	ΔE_{total}	$\Delta E^{\ddagger}$	E_{total}	ΔE_{total}	$\Delta E^{\ddagger}$
CPR[b]	−117.897 878	0.00	0.00	−117.544 380	0.00	0.00	−117.084 033	0.00	0.00
TS1	−117.803 159	59.44	53.87	−117.446 338	61.52	55.95	−117.000 640	52.33	46.89
TS2	−117.801 333	60.58	55.19	−117.446 338	62.01	56.62	−116.999 842	52.83	47.91
TS3/*T3*[c]	−117.801 077	60.74	55.21	−117.445 315	62.16	56.63	−116.998 935	53.40	48.35
INT	−117.803 368	59.31	53.92	−117.446 694	61.30	55.91	−117.001 482	51.80	47.07
TS4	−117.787 546	69.23	63.58	−117.431 672	70.73	65.08	−116.972 241	70.15	64.37
TS5[d]	−117.708 929	118.57	111.30	−117.360 548	115.36	107.92			

[a] $\Delta E^{\ddagger} = \Delta E_{total} + \Delta(ZPE)$. [b] Cyclopropane. [c] TS3 from TCSCF and T3 from uB3LYP and uQCISDT calculations. [d] Shows Hartree−Fock instability.

TABLE 9: Total Energies E_{total} (a.u.) and Relative Energies[a] (in Parentheses, kcal/mol) of Trimethylene Species, Obtained in This and Previous Investigations

method/species	INT	TS1	TS2	TS3/*T3*[b]
Baldwin et al.[8]				
TCSCF/6-31G*[c]	−116.989696 (0.0)	−116.989538 (0.10)	−116.988759 (0.59)	−116.987686 (1.26)
TCSCF/DZP[c]	−117.016721 (0.0)	−117.016660 (0.04)	−117.015807 (0.57)	−117.014936 (1.12)
CISD/6-31G*[d]	−117.342140 (0.0)	−117.342523 (−0.24)	−117.340999 (0.72)	−117.340826 (0.82)
CISD+Q/6-31G*[e]	−117.380360 (0.0)	−117.380855 (−0.31)	−117.379151 (0.76)	−117.379364 (0.62)
CISD/DZP	−117.399357 (0.0)	−117.399493 (−0.09)	−117.398282 (0.67)	−117.398016 (0.84)
CISD+Q/DZP	−117.443405 (0.0)	−117.443576 (−0.11)	−117.442290 (0.70)	−117.442355 (0.66)
Doubleday[13f]				
2,2-CAS/VTZ(2d,p)	−117.028264 (0.0)	−117.028258 (0.004)	−117.026723 (0.97)	−117.025868 (1.50)
CISD//2,2-CAS/VTZ(2d,p)	−117.446177 (0.0)	−117.446386 (−0.13)	−117.444220 (1.23)	−117.443209 (1.86)
this investigation				
TCSCF/cc-pVDZ	−117.001482 (0.0)	−117.000640 (0.53)	−116.999842 (1.31)	−116.998935 (1.60)
uB3LYP/cc-pVDZ	−117.803368 (0.0)	−117.803159 (0.13)	−117.801333 (1.28)	−117.801077 (1.44)
uQCISD(T)/cc-pVDZ	−117.446694 (0.0)	−117.446338 (0.22)	−117.445566 (0.71)	−117.445313 (0.87)

[a] Values are without ZPE correction. [b] TS3 from TCSCF and T3 from uB3LYP and uQCISD(T) calculations. [c] The geometry optimization were carried out using the TCSCF analytical first-derivative method.[36] [d] The configuration interactions with single- and double-excitation (CISD) energies were determined at the SCF-optimized geometry.[37] [e] The Davidson's correction was applied to estimate approximately unlinked quadruple excitations. [f] Relative enegries with respect to intermediate 1.

In contrast to the trimethylene intermediate and the geometrical and optical transition states, which are 1,3 biradicals, the structural transition states TS4 is a closed-shell singlet with only some biradical character. The wave function from TCSCF calculations of this trimethylene consists of the following configurations: 110 = 0.370, 200 = 0.840, and 020 = 0.275**,** as previously defined. The electron occupation numbers of the orbitals are 1.61 and 0.39, which means that the α-orbital is almost doubly occupied. This orbital reflects the early stages of formation of a π-bond between C(1) and C(2) and a σ-bond between H(1) and C(3). For comparison, the electron occupation numbers of the α and β single occupied orbitals in the geometrical manifold are 1.11, 0.89 in TS1; 1.12, 0.88 in TS2; 0.95, 1.05 in TS5, and 1.10, 0.90 in the intermediate. Table 6 shows that α and β atomic spin densities on the terminal carbon atoms are smaller than in the intermediate and TS1 and TS2. Also, $\langle S^2 \rangle$ shows considerably less spin contamination in TS4 (Table 7). On the other hand, the dipole moment of TS4 (Table 7), which is the highest among the trimethylene conformers, indicates a high contribution of an ionic term to its wave function. Thus the analysis of the dipole moments and wave functions shows that the transition state of the structural isomerization is a polar structure with some contribution of biradical configuration in contradiction to the geometrical transition states, which are definitely 1,3-biradicals.

The activation barrier of the structural isomerization calculated at all levels of theory (Table 8) is in agreement with the experimental values which range between 62 and 67 kcal/mol at different temperatures.[38−42]

Our calculated transition state TS4 is very similar, both in energy and structure, to the transition state 5 in Doubleday's[13] calculations. However our IRC analysis using uB3LYP shows that TS4 goes directly to cyclopropane rather than to an intermediate as was calculated by Doubleday. This disagreement is not surprising since the potential energy surface is very shallow. It should be mentioned that in our study of the isomerization of cyclopropanecarbonitrile[43] we did find an intermediate in the stepwise manifold using the uB3LYP method, a fact that indicates that the use of this method was not the reason for not finding the intermediate in the cyclopropane structural isomerization.

We found an additional transition state, TS5, which corresponds to a concerted mechanism and it is a nonradical, closed-shell specie. The transition state is shown in Figure 4 and its geometrical parameters are given in Table 3. The ring opening in TS5, which expresses itself by the r-C(2)C(3) distance and the C(2)C(2)C(3) angle, is less pronounced than in TS4. These parameters are 2.35 Å and 113° in TS5 compared to 2.61 Å and 128° in TS4. The reaction coordinate is an asymmetric stretch of the ring carbon and 1,2-H-atom shift from C(1) to C(2) but not quite in the same manner as in TS4. It is a zwitterion or 1,3-dipole structure (see Table 7).

The reaction, which could proceed via TS5, does not add any substantial contribution to over-all rate owing to the very high energy barrier (Table 8). It should also be mentioned that TS5 shows Hartree−Fock instability at B3LYP level and thus its physical significance is somewhat questionable.

Comparison with Experimental Results on the Structural Isomerization of Cyclopropane. There is a large volume of experimental data on the isomerizations of cyclopropane. In the early study of Rabinovitch et al.[38] a rate constant of $k = 10^{15.2} \exp(-65.5 \times 10^3/RT)\ s^{-1}$ was reported for the structural isomerization and $k = 10^{16.0} \exp(-64.2 \times 10^3/RT)\ s^{-1}$ for the geometrical isomerization. In an additional study by Waage

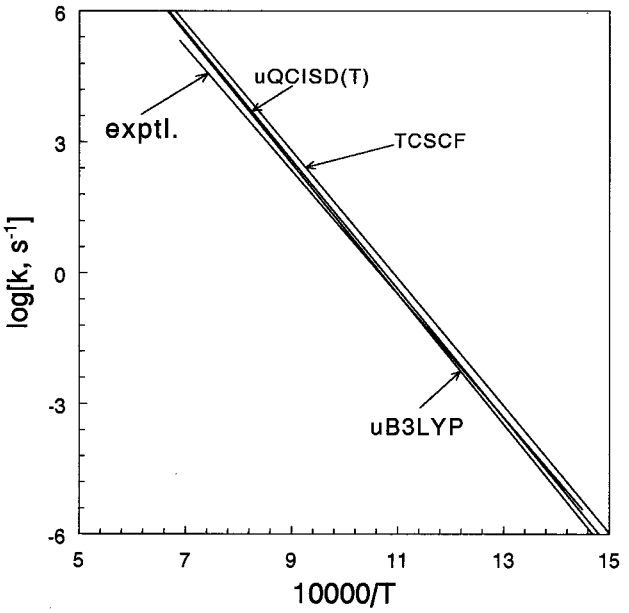

Figure 5. Arrhenius plots of the experimental[42] and calculated rate constants of the structural isomerization of cyclopropane for different methods of calculation.

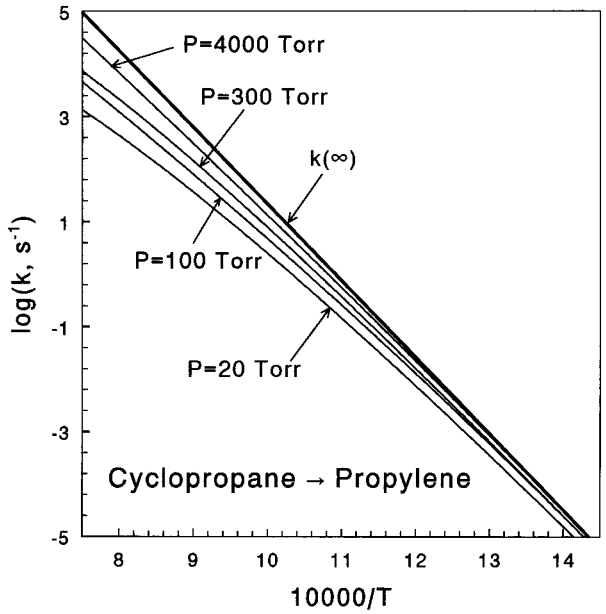

Figure 6. Arrhenius plots of the uB3LYP calculated rate constants for the structural isomerization of cyclopropane at different pressures as obtained by RRKM calculations.

and Rabinovith,[42] a value of 3.7 kcal/mol was reported for the difference between the structural and the geometrical isomerizations. Whereas both the activation energies and preexponential factors varied from one study to another, it was evident that at temperatures where both isomerizations were studied i.e., around 500 °C the geometrical isomerization was about 10−20 times faster than the structural isomerization.

To evaluate the high-pressure limit first-order rate constant from our quantum chemical calculations the relation

$$k_\infty = \sigma(kT/h)\exp(\Delta S^{\ddagger}/R)\exp(-\Delta H^{\ddagger}/RT)$$

was used,[44,45] where h is Planck constant, k is Boltzmann constant, σ is the degeneracy of the reactional coordinate (12 for the structural isomerization of cyclopropane), and $\Delta H^{\ddagger}$ and $\Delta S^{\ddagger}$ are the enthalpy and entropy of activation, respectively. Since we deal with isomerizations where there is no change in the number of moles $\Delta H^{\ddagger} = \Delta E^{\ddagger}$, where $\Delta E^{\ddagger}$ is the energy difference between the transition state and the reactant. $\Delta E^{\ddagger}$ is equal to $\Delta E^0_{\text{total}} + \Delta(\text{ZPE})$, where $\Delta E^0_{\text{total}}$ is obtained by taking the difference between the total energies of the transition state and the reactant, and Δ(ZPE) is the difference between ZPE of these species. Calculated entropies and zero point energies are shown in Table 7 and total energies and $\Delta E^{\ddagger}$ in Table 8.

For comparison with the experimental rate parameters (A and E_a), we replaced $\Delta E^{\ddagger}$ by E_a, where $E_a = \Delta E^{\ddagger} + RT$ and used the relation, $k_\infty = \sigma(ekT/h)\exp(\Delta S^{\ddagger}/R)\exp(-E_a/RT)$, where A is given by $A = \sigma(ekT/h)\exp(\Delta S^{\ddagger}/R)$.

On the basis of our calculated energies (Table 8) and the molecular parameters (Table 7), we evaluated the preexponential factors and activation energies for the structural isomerization using the above relation. The values obtained for A are $10^{12.11}T$ at uB3LYP and $10^{12.04}T$ s^{-1} at TCSCF levels of theory and the activation energies are 63 580 + RT, 65 080 + RT, and 64 370 + RT cal/mol at uB3LYP, uQCISD(T), and TSCSF levels, respectively. Figure 5 shows a comparison between the calculated rate constants and the experimental value as obtained by a best fit to the data on cyclopropane → propylene isomerization taken from NIST chemical kinetics database.[46] As can be seen, the agreement is very good. In terms of an Arrhenius rate expression, the calculated (uB3LYP) high-pressure limit rate constant for the isomerization is given by $k_\infty = 10^{15.91}\exp(-66.7 \times 10^3/RT)\text{sec}^1$.

Figure 6. shows the results of RRKM calculations done for different temperatures and pressures using the results obtained at the uB3LYP level of theory. The RRKM calculations employed the standard routine,[47] which uses a direct vibrational state count with classical rotation for the transition state. The path degeneracy σ was set equal to 12. The threshold energy is 63 580 cal/mol and $\langle E_{\text{down}}\rangle = 600$ cm^{-1}.

The Arrhenius expressions for different pressures in the temperature range 900−1300 K as obtained by the RRKM calculations are $10^{11.85}\exp(-52.6 \times 10^3/RT)$, $10^{12.69}\exp(-55.0 \times 10^3/RT)$, $10^{13.28}\exp(-56.9 \times 10^3/RT)$, and $10^{14.57}\exp(-61.5 \times 10^3/RT)$ s^{-1} for 20, 100, 300, and 4000 Torr, respectively. At 1000 K, this corresponds to factors of 0.1, 0.2, 0.3, and 0.6 lower than k_∞ at 20, 100, 300, and 4000 Torr respectively.

Conclusions

Quantum chemical calculations on cyclopropane using the density functional theory B3LYP method with the cc-pVDZ basis set reproduce very well its experimental structural parameters and vibrational frequencies. With this basis set and uB3LYP, uQCISD(T), and TCSCF methods, the energy levels of the transition states for the different pathways of the geometrical isomerization are in good agreement with previous calculations. A transition state for the structural isomerization was calculated with the aforementioned method, and its parameters and vibrational frequencies are reported. According to our calculations, the structural isomerization proceeds via a concerted mechanism with no intermediate, but owing to a very shallow potential energy surface, the exact mechanism is still an open question. Very good agreement between the calculated Arrhenius parameters and the experimental values was obtained.

Acknowledgment. The authors thank the Ministry of Absorption for a fellowship to F.D.

References and Notes

(1) Berson, J. A. In *Rearrangements in ground and exited states*; de Mayo, P., Ed.; Academic Press: New York, 1980; Vol. 1, p 311.

(2) Benson, S. W. *Thermochemical kinetics. Methods for the estimation of thermochemical data and rate parameters*; A Wiley-Interscience Publ.: New York, 1976; p 117.
(3) Bergman, R. G. In *Free Radicals*; Wiley-Interscience Publ.: New York, 1973; Vol. 1, p 191.
(4) Laidler, K. J.; Loucks L. F. In *Comprehensive chemical kinetics*; Bamford, C. H., Tipper, C. F. H., Eds.; Elsevier Publishing Co.: Amsterdam, 1972; Vol. 5, p 1.
(5) Hoffman, R. *J. Am. Chem. Soc.* **1968**, *90*, 1475.
(6) Kato, S.; Morokuma, K. *Chem. Phys. Lett.* **1979**, *65*, 19.
(7) Yamaguchi, Y.; Schaefer, H. F., III.; Baldwin, J. E. *Chem. Phys. Lett.* **1991**, *185*, 143.
(8) Baldwin, J. E.; Yamaguchi, Y.; Schaefer, H. F., III *J. Phys. Chem.* **1994**, *98*, 7513.
(9) Hayes, E. F.; Siu, A. K. Q. *J. Am. Chem. Soc.* **1971**, *93*, 2090.
(10) Horsley, J. A.; Jean, Y.; Moser, C.; Salem, L.; Stevens, R. M.; Wright, J. S. *J. Am. Chem. Soc.* **1972**, *94*, 279.
(11) Hay, P. J.; Hunt, W. J.; Goddard, W. A. *J. Am. Chem. Soc.* **1972**, *94*, 638.
(12) Getty, S. S.; Davidson E. R.; Borden, W. T. *J. Am. Chem. Soc.* **1992**, *114*, 2085.
(13) Doubleday, C., Jr. *J. Phys. Chem.* **1996**, *100*, 3520.
(14) Jug, K. *Theor. Chem. Acta* **1976**, *42*, *303.*
(15) Slater, N. B. *Proc. R. Soc. (London) Ser. A* **1953,** *218*, 224.
(16) Lin, M. C.; Laidler, K. J. *Trans. Faraday Soc.* **1968**, *64*, 94.
(17) Blades, A. T. *Can. J. Chem.* **1961**, *39*, 1401.
(18) Wieder, G. M.; Marcus, R. A. *J. Chem. Phys.* **1962**, *37*, 1835.
(19) Benson, S. W.; Nagia, P. S. *J. Chem. Phys.* **1963**, *38*, 18.
(20) Benson, S. W. *J. Chem. Phys.* **1961**, *34*, 521.
(21) Luckruft, D. A.; Robison, P. J. *Int. J. Chem. Kinet.* **1973**, *5*, 137.
(22) Lifshitz, A.; Shweky, J. H.; Kiefer J. H.; Sidhu, S. S. In *Shock Waves*; Proceeding in the 18th Int. Symposium on Shock Waves, Sendia, Japan, 1991, Takayama, K., Ed.; Springer-Verlag: Berlin, 1992; p 825.
(23) Becke, A. D. *J. Chem. Phys.* **1993**, *98*, 5648.
(24) Lee, C.; Yang, W.; Parr, R. G. *Phys. Rev.* **1988**, *B37*, 785.
(25) Frisch, M. J.; Trucks, G. W.; Schlegel, H. B.; Gill, P. M. W.; Johnson, B. G.; Robb, M. A.; Cheeseman, J. R.; Keith, T.; Petersson, G. A.; Montgomery, J. A.; Rahavachari, K.; Al-Laham, M. A.; Zakrzewski, V. G.; Orviz, J. V.; Foresman, J. B.; Cioslowski, J.; Stefanov, B. B.; Nanayakkara, A.; Challacombe, M.; Peng, C. Y.; Ayala, P.Y.; Chen, W.; Wong, M. W.; Andres, J. L.; Replogle, E. S.; R. Gomperts, R.; Martin, R. L.; Fox, D. J.; Binkley, J. S.; Defrees, D. J.; Baker, J.; Stewart, J. P.; Head-Gordon, M.; Gonzalez, C.; Pople, J. A. *GAUSSIAN* 94, *Revision* B.1, Gaussian, Inc., Pittsburgh, 1995.
(26) Hehre, W. J.; Detchfield, R. D.; Pople, J. A. *J. Chem. Phys.* **1972**, *56*, 2257.
(27) Dunning, T. H., Jr. *J. Chem. Phys.* **1989**, *90*, 1007.
(28) Kendall, R. A.; Dunning, T. H., Jr.; Harrison, R. J. *J. Chem. Phys.* **1992**, *96*, 6796.
(29) Pople, J. A.; Head-Gordon, M.; Raghavachari, K. *J. Chem. Phys*, **1987**, *87*, 5968.
(30) Doubleday, C., Jr.; McIver, J., Jr.; Page, M. *J. Am. Chem. Soc.* **1982**, *104*, 6533.
(31) GAMESS−USA, Revision Mar. 1997; Schmidt M. W.; Baldridge, K. K.; Boatz, J. A.; Elbert, S. T.; Gordon, M. S.; Jensen, J. H.; Koseki, S.; Matsunaga, N.; Nguyen, K. A.; Su, S. J.; Windus, T. L.; Dupuis, M.; Montgomery, J. A. See, for example: Schmidt M. W.; Baldridge, K. K.; Boatz, J. A.; Elbert, S. T.; Gordon, M. S.; Jensen, J. H.; Koseki, S.; Matsunaga, N.; Nguyen, K. A.; Su, S. J.; Windus, T. L.; Dupuis, M.; Montgomery, J. A. *J. Comput. Chem.* **1993**, *14*, 1347.
(32) Shaik, S. S.; Schlegel, H. B.; Walfe, S. *Theoretical Aspects of Physical Organic Chemistry the SN2 Mechanism*; Wiley: New York, 1992; p 45.
(33) Yamamoto, S.; Nakata, M.; Fukuyama, T.; Kuchitsu, K. *J. Phys. Chem.* **1985**, *89*, 3298.
(34) Duncon, J. L.; Burns, G. R. *J. Mol. Spectrom.* **1969**, *30*, 253.
(35) Wong, M. W. *Chem. Phys. Lett.* **1996**, *256*, 391.
(36) Goddard, J. D.; Handy, N. C.; Schaefer, H. F. *J. Chem. Phys.* **1979**, *71*, 1525.
(37) Osamura, Y.; Yamaguchi, Y.; Schaefer, H. F. *J. Chem. Phys.* **1982**, *77*, 383.
(38) Rabinovitch, B. S.; Schlag, E. M.; Wiberg, K.B. *J. Chem. Phys.* **1958**, *28*, 504.
(39) Schlag, E. M.; Rabinovitch, B. S. *J. Am. Chem. Soc.* **1960**, *82*, 599.
(40) Langrish, J.; Prichard, H. O. *J. Chem. Phys.* **1958**, *26*, 761.
(41) Tsang, W. Comparative-rate single-pulse shock tube studies on the thermal stability of polyatomic molecules In *Shock waves in chemistry*; Lifshtz, A., Ed., Marcel Dekker inc., New York, 1981; p 115.
(42) Waage, E. V.; Rabinovitch, B. S. *J. Phys. Chem.* **1972**, *76*, 1695.
(43) Dubnikova, F.; Lifshitz, A. Unpublished results.
(44) Eyring, H. *J. Chem. Phys.* **1935**, *3*, 107.
(45) Evans, M. G.; Polanyi, M. *Trans. Faraday Soc.* **1935**, *31*, 875.
(46) Westly, F.; Herron, J. T.; Cvetanovich, R. J.; Hampson, R. F.; Mallard, W.G. NIST-Chemical Kinetics Standard Reference Data Base 17, ver. 6.
(47) Kiefer, J. H.; Shah, J. N. *J. Phys. Chem.* **1987**, *91*, 3024.